Comparison among the FEM, the SEM and a Bessel-based dynamic stiffness method for tapered beams discretization purposes

Alberto Coronado-Matutti

Departamento de Engenharia Mecânica, PUC–Rio, Rua Marquês de São Vicente 225, 22453–900, Rio de Janeiro, Brazil, beto_cm@yahoo.com

Rubens Sampaio

Departamento de Engenharia Mecânica, PUC–Rio, Rua Marquês de São Vicente 225, 22453–900, Rio de Janeiro, Brazil, rsampaio@mec.puc–rio.br

Abstract. *Tapered beams have many practical uses and their importance is clearly shown, for example, when used as an efficient weight saving methodology in applications such as aeronautical structures. Structural optimization taking into account the beams cross-section variation has produced noticeable response improvements. Even so, the calculation of the system response poses a difficult problem since it may be very time consuming and/or little reliable. Vibrational power considers all the relevant variables in dynamic systems response, so it was used as a comparison measure here. In this paper, the tapered leg of a T-beam structure was discretized using three different methods. The first, the Finite Element Method (FEM) that is widely used with dynamic analysis purposes because of its general character. Nevertheless, the use of the FEM has many drawbacks like the high computational cost and the loss of confidence at high frequencies. Additionally, the derivation of mass and stiffness element matrices for tapered Timoshenko beams is a laborious task, even more for a two-node element. So, in order to overcome this problem, it was considered a four-node element, which was reduced to a two-node element using the Guyan static condensation. The second, the Spectral Element Method (SEM) was used to obtain an approximate dynamic stiffness matrix for tapered Timoshenko beams, but this solution is not reliable for coarse meshes. Finally, the Bessel functions were used to obtain the exact dynamic stiffness matrix of tapered Euler-Bernoulli beams. The results showed that the Bessel-based method is not suitable to calculate the frequency response and only predicts properly the resonance frequencies. After comparing the responses obtained by the three methods above mentioned, the SEM showed the best features, it was at least two times faster than the FEM and more suitable for discretization than the Bessel-based method.*

Keywords: *tapered beams, spectral element method, power flow.*

1   Introduction

Optimization techniques are used in structural projects that require a great improvement in the system original configuration and/or performance (Langthjem & Sugiyama, 1999). Structural optimization usually requires complex computer simulations. So, in order to keep the computing effort at reasonable levels it is important to take into account all the measures that could be useful to save time processing. This saving could be achieved, for example, choosing the most suitable discretization method. The size of the matrices related to the discretized system, and so the computing effort too, will depend strongly on this selection (Coronado-Matutti, 2003).

In the last years, the development of search techniques based on evolutionary concepts, like the genetic algorithms for example, required to carry out even millions of simulations in order to choose the best structural configuration. In this environment, a careful selection of the discretization method is a critical issue and even a minimum improvement will be very helpful.

As a general purpose, this paper intends to put forward an alternate discretization method to the widely used Finite Element Method (FEM) that could be useful in some specific applications.

Engineering problems involving dynamic analysis of structures can, in general, be solved using a conventional methodology like the Finite Element Method (FEM) (Bathe, 1996), which represents the structure as a junction of simple elements like bars, beams, plates, etc. The approximate response at each point is calculated using in conjunction shape functions and techniques such as variational methods. Although this procedure is usually adequate, there are situations in which it becomes inefficient, for example in the dynamic analysis at high frequencies or when the spatial distribution of the loads is highly non-uniform.

Alternate methodologies to the FEM are the Spectral Element Method (SEM) (Doyle, 1997) and the Bessel-based method, in which, sometimes, the dynamic stiffness matrices of the structural elements can be exactly derived from the differential equations of motion. This means that every member in the structure can be discretized using only one element disregarding the level of the excitation frequency.

2 The Finite Element Method (FEM)

There are many finite element models of rods and beams which were developed in the last four decades. Besides, the derivation of mass and stiffness matrices became an easier task after the popularization of symbolic processing software.

The Timoshenko beam, in special, attracted from the beginning considerable attention due to the difficulty to derive suitable mass and stiffness matrices and, chiefly, to the existence of drawbacks related to the finite element formulation, like the shear locking. Moreover, it is hard to define a suitable value for the shear correction factor, which depends on many variables, among them, in dynamic problems, the excitation frequency.

In this work, the mass and the stiffness matrices of linearly tapered Timoshenko beams are derived. The traditional approximations, which consider two nodes (four-degrees-of-freedom) (Davis et al, 1972; Dawe, 1978) lead to unsuitable expressions. To tackle this problem, it was applied the Guyan static condensation (Corn et al, 1997) to a four node (eight-degrees-of-freedom) beam element (Corn et al, 1997; Rao & Gupta, 2001; Yokoyama, 1994) to obtain a two node (four-degrees-of-freedom) beam element.

2.1 Timoshenko beam element

Considering a tapered Timoshenko beam as a simplification of a plane stress state, the kinetic energy T_b is given by

$$
\begin{aligned}
T_b &= \int_\forall \frac{1}{2}\rho \left(\dot{\bar{u}}(x,y,t)^2 + \dot{\bar{v}}(x,y,t)^2\right) d\forall \\
&\approx \frac{1}{2}\int_0^L \left(\rho I(x)K_2\dot{\theta}(x,t)^2 + \rho A(x)\dot{v}(x,t)^2\right) dx
\end{aligned}
\tag{1}
$$

and the elastic energy U_b by

$$
\begin{aligned}
U_b &= \int_\forall \frac{1}{2}\left(\bar{\sigma}_{xx}(x,y,t)\bar{\epsilon}_{xx}(x,y,t) + \bar{\sigma}_{xy}(x,y,t)\bar{\gamma}_{xy}(x,y,t)\right) d\forall \\
&\approx \frac{1}{2}\int_0^L \left(EI(x)\left(\frac{\partial\theta(x,t)}{\partial x}\right)^2 + GA(x)K_1\left(\frac{\partial v(x,t)}{\partial x} - \theta(x,t)\right)^2\right) dx
\end{aligned}
\tag{2}
$$

ρ is the density, u the longitudinal displacement, v the transversal deflexion, θ the bending rotation, L the beam total length, A the cross-section area, I the cross-section second moment of area, σ_{xx} and ϵ_{xx} the longitudinal stress and strain respectively, σ_{xy} and γ_{xy} the shear stress and strain respectively, K_1 is the shear correction factor and K_2 is the rotation inertia coefficient. In this work, $K_1 = \pi/12$ (Mindlin coefficient) and $K_2 = 1$. The overlined dependent variables refer to the plane stress state.

The potential function V_b due to external applied loads at the beam ends is

$$
V_b = -M_L\phi_L + M_0\phi_0 - V_Lv_L + V_0v_0 = -\left.M\theta\right|_0^L - \left.Vv\right|_0^L
\tag{3}
$$

The above expressions for T_b, U_b and V_b are used in the Hamilton equation

$$
\delta\int_{t_1}^{t_2}\left(T_b - (U_b + V_b)\right) dt = 0
\tag{4}
$$

Discretizing the beam of length L in n four-node beam elements of length l, Fig. 1.

The nodal variables used are the transversal deflexion v and the bending rotation θ, Fig. 2. Since the element has eight-degrees-of-freedom, the nodal displacements vector is given by $\mathbf{q}^e = [v_1 \ \theta_1 \ v_2 \ \theta_2 \ v_3 \ \theta_3 \ v_4 \ \theta_4]^T$, the subscripts $1-4$ refer to the local node number. Considering the two nodal variables v and θ as totaly independent (Yokoyama, 1994)

$$
v(x,t) = [N_1(x) \ N_2(x) \ N_3(x) \ N_4(x)][v_1 \ v_2 \ v_3 \ v_4]^T
\tag{5}
$$

$$
\theta(x,t) = [N_1(x) \ N_2(x) \ N_3(x) \ N_4(x)][\theta_1 \ \theta_2 \ \theta_3 \ \theta_4]^T
\tag{6}
$$

$N_1(x) = -\frac{(3x-L)(3x-2L)(3x-3L)}{6L^3}$, $N_2(x) = \frac{3x(3x-2L)(3x-3L)}{2L^3}$, $N_3(x) = -\frac{3x(3x-L)(3x-3L)}{2L^3}$ and $N_4(x) = \frac{3x(3x-L)(3x-2L)}{6L^3}$ are cubic interpolation functions.
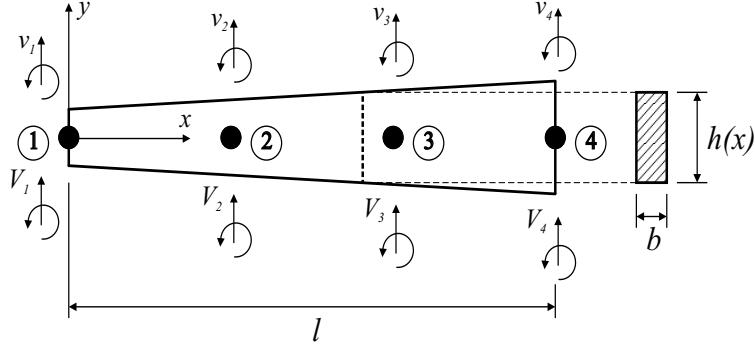
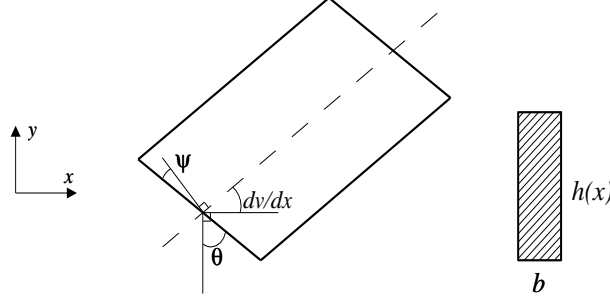Figure 1. Four-node Timoshenko beam element.

Figure 2. Variables in the Timoshenko beam.

Applying the Ritz approximation (Reddy, 1984) to the elementary version of the Hamilton equation to obtain the element mass $\mathbf{M}^e$ and stiffness $\mathbf{K}^e$ matrices

$$\mathbf{M}^e = \int_0^l \mathbf{N}_\theta^T \rho I K_2 \mathbf{N}_\theta dx + \int_0^l \mathbf{N}_v^T \rho A \mathbf{N}_v dx \tag{7}$$

$$\mathbf{K}^e = \int_0^l \mathbf{B}_b^T E I \mathbf{B}_b dx + \int_0^l \mathbf{B}_s^T G A K_1 \mathbf{B}_s dx \tag{8}$$

E is the Young's modulus, G is the shear modulus, $\mathbf{N}_v = [N_1 \ 0 \ N_2 \ 0 \ N_3 \ 0 \ N_4 \ 0]$ and $\mathbf{N}_\theta = [0 \ N_1 \ 0 \ N_2 \ 0 \ N_3 \ 0 \ N_4]$. The strain due to the bending moment is $\epsilon_b = d\theta/dx$, likewise the strain due to the shear stress is $\epsilon_s = \psi = dv/dx - \theta$. The generalized strain-displacement relationships are $\epsilon_b = \mathbf{B}_b \mathbf{q}^e$ and $\epsilon_s = \mathbf{B}_s \mathbf{q}^e$. The strain-displacement vectors due to the bending moment and the shear stress, respectively, are

$$\mathbf{B}_b = \begin{bmatrix} 0 & \dfrac{dN_1}{dx} & 0 & \dfrac{dN_2}{dx} & 0 & \dfrac{dN_3}{dx} & 0 & \dfrac{dN_4}{dx} \end{bmatrix} \tag{9}$$

$$\mathbf{B}_s = \begin{bmatrix} \dfrac{dN_1}{dx} & -N_1 & \dfrac{dN_2}{dx} & -N_2 & \dfrac{dN_3}{dx} & -N_3 & \dfrac{dN_4}{dx} & -N_4 \end{bmatrix} \tag{10}$$

Furthermore, the cross-section area and the cross-section second moment of area are $A(x) = A_1 \left(1 + \frac{\delta x}{L}\right)$ and $I(x) = I_1 \left(1 + \frac{\delta x}{L}\right)^3$, respectively. The subscript 1 refers to node 1 (Fig. 1).

$\mathbf{M}^e$ and $\mathbf{K}^e$ are $[8 \times 8]$ element matrices. In order to obtain $[4 \times 4]$ element matrices, the degrees of freedom are divided in 2 subsets: *masters*, related to the end nodes (1 and 4) and *slaves*, related to the internal nodes (2 and 3). So, the nodal displacements vector can be rearranged as $\mathbf{q}^e = [\mathbf{q}_m \ \mathbf{q}_s]^T$ with $\mathbf{q}_m = [v_1 \ \theta_1 \ v_4 \ \theta_4]^T$ and $\mathbf{q}_s = [v_2 \ \theta_2 \ v_3 \ \theta_3]^T$. Likewise, the element mass and stiffness matrices are

$$\mathbf{M}^e = \begin{bmatrix} \mathbf{M}_{mm} & \mathbf{M}_{ms} \\ \mathbf{M}_{ms}^T & \mathbf{M}_{ss} \end{bmatrix}, \quad \mathbf{K}^e = \begin{bmatrix} \mathbf{K}_{mm} & \mathbf{K}_{ms} \\ \mathbf{K}_{ms}^T & \mathbf{K}_{ss} \end{bmatrix} \tag{11}$$

The dynamic equilibrium equation for a rearranged Timoshenko beam element is $[\mathbf{K}^e - \omega^2 \mathbf{M}^e]\mathbf{q}^e = \mathbf{F}^e$, with $\mathbf{F}^e = [\mathbf{F}_m \ \mathbf{0}]^T$, the interelementar forces vector.

Using the Guyan static condensation for the nodal displacements vector (Corn et al, 1997)

$$\mathbf{q}^e = \underbrace{\begin{bmatrix} \mathbf{I}_m \\ -\mathbf{K}_{ss}^{-1}\mathbf{K}_{ms}^T \end{bmatrix}}_{\mathbf{T}_G} \mathbf{q}_m \tag{12}$$

$\mathbf{I}_m$ is an $[m \times m]$ identity matrix. Then, the dynamic equilibrium equation in the condensed form is $[\mathbf{K}_c^e - \omega^2 \mathbf{M}_c^e]\mathbf{q}_m = \mathbf{F}_m$, with

$$\mathbf{M}_c^e = \mathbf{T}_G^T \mathbf{M}^e \mathbf{T}_G, \quad \mathbf{K}_c^e = \mathbf{T}_G^T \mathbf{K}^e \mathbf{T}_G \tag{13}$$

$\mathbf{M}_c^e$ and $\mathbf{K}_c^e$ are $[4 \times 4]$ matrices condensed in the boundary degrees of freedom. So, the element mass and stiffness matrices used in the numerical simulations are

$$\mathbf{M}_b^e = \mathbf{M}_c^e, \quad \mathbf{K}_b^e = \mathbf{K}_c^e \tag{14}$$

3 The Spectral Element Method (SEM)

An efficient way to solve wave propagation problems in complex structures is using a matricial method. The SEM is very similar to the FEM, but the SEM has as a principal advantage to be formulated in the frequency domain, this leads to an exact description of the inertia of the distributed mass. So, sometimes it is possible to obtain spectral elements that describe exactly the structural dynamics. In this work, it will be derived only an approximate dynamic stiffness matrix for tapered Timoshenko beams.

3.1 Timoshenko beam element

From the Hamilton equation it is possible to obtain the differential equations that describe the displacements in a Timoshenko beam of constant cross-section (Doyle, 1997)

$$GA_1 K_1 \frac{\partial}{\partial x}\left(\frac{\partial v(x,t)}{\partial x} - \theta(x,t)\right) = \rho A_1 \frac{\partial^2 v(x,t)}{\partial t^2}$$
$$EI_1 \frac{\partial^2 \theta(x,t)}{\partial x^2} + GA_1 K_1 \left(\frac{\partial v(x,t)}{\partial x} - \theta(x,t)\right) = \rho I_1 K_2 \frac{\partial^2 \theta(x,t)}{\partial t^2} \tag{15}$$

where v is the transversal deflection, θ is the bending rotation, A_1 is the cross-section area, I_1 is the second moment of area, E is the Young's modulus, G is the shear modulus, ρ is the material density, K_1 is the shear correction factor and K_2 is the rotation inertia coefficient.

There are two independent variables v and θ. Assuming the solutions $v(x,t) = v_0 e^{-i(kx-\omega t)}$ and $\theta(x,t) = \theta_0 e^{-i(kx-\omega t)}$. Then, after substituting them into Eq. 15, it is obtained

$$\begin{bmatrix} GA_1 K_1 k^2 - \rho A_1 \omega^2 & -ikGA_1 K_1 \\ ikGA_1 K_1 & EI_1 k^2 + GA_1 K_1 - \rho I_1 K_2 \omega^2 \end{bmatrix} \begin{bmatrix} v_0 \\ \theta_0 \end{bmatrix} = 0 \tag{16}$$

which gives the characteristic equation

$$\left(\frac{EI_1}{\rho A_1}\right) k^4 - \left(\frac{EI_1 \omega^2}{GA_1 K_1} + \frac{\rho I_1 K_2 \omega^2}{\rho A_1}\right) k^2 + \left(\frac{\rho I_1 K_2 \omega^4}{GA_1 K_1} - \omega^2\right) = 0 \tag{17}$$

There are four roots, the wavenumbers $\pm k_1$ and $\pm k_2$. The transversal deflection v and the bending rotation θ in the frequency domain are given by

$$\hat{v}(x) = R_1 \widetilde{A} e^{-ik_1 x} + R_2 \widetilde{B} e^{-ik_2 x} - R_1 \widetilde{C} e^{-ik_1(L-x)} - R_2 \widetilde{D} e^{-ik_2(L-x)}$$
$$\hat{\theta}(x) = \widetilde{A} e^{-ik_1 x} + \widetilde{B} e^{-ik_2 x} + \widetilde{C} e^{-ik_1(L-x)} + \widetilde{D} e^{-ik_2(L-x)} \tag{18}$$

$\widetilde{A}$, $\widetilde{B}$, $\widetilde{C}$ and $\widetilde{D}$ are boundary dependent coefficients. R_1 and R_2 are amplitude ratios. The displacements $\hat{v}(x)$ and $\hat{\theta}(x)$ can be expressed in function of the nodal displacements $\hat{v}_1$, $\hat{\theta}_1$, $\hat{v}_2$ and $\hat{\theta}_2$, instead of the coefficients $\widetilde{A}$, $\widetilde{B}$, $\widetilde{C}$ and $\widetilde{D}$

$$\hat{v}(x) = \hat{\mathbf{N}}_b^T \hat{\mathbf{L}}_1 \hat{\mathbf{G}}_b \hat{\mathbf{q}}_b^e, \quad \hat{\theta}(x) = \hat{\mathbf{N}}_b^T \hat{\mathbf{G}}_b \hat{\mathbf{q}}_b^e \tag{19}$$

$\hat{\mathbf{G}}_b$ is a $[4 \times 4]$ matrix that relates two vectors, $[\widetilde{A} \quad \widetilde{B} \quad \widetilde{C} \quad \widetilde{D}]^T = \hat{\mathbf{G}}_b \underbrace{[\hat{v}_1 \quad \hat{\theta}_1 \quad \hat{v}_2 \quad \hat{\theta}_2]^T}_{\hat{\mathbf{q}}_b^e}$.

Moreover, $\hat{\mathbf{N}}_b^T = \begin{bmatrix} e^{-ik_1x} & e^{-ik_2x} & e^{-ik_1(L-x)} & e^{-ik_2(L-x)} \end{bmatrix}$ and $\hat{\mathbf{L}}_1 = diag[R_1 \quad R_2 \quad -R_1 \quad -R_2]$.

The displacements v and θ of a tapered Timoshenko beam element (Fig. 3) can be approximated using the displacements of a constant cross-section beam (Eq. 19). So, using l instead of L.
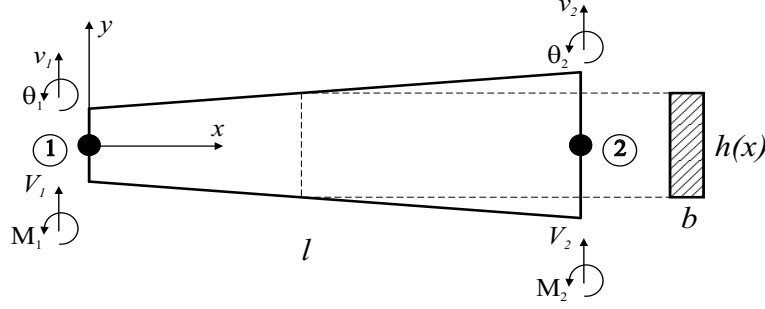

Figure 3. Tapered Timoshenko beam element with two nodes.

The kinetic $\hat{T}_b^e$ and strain $\hat{U}_b^e$ energy equations of a Timoshenko beam element in the frequency domain are (Doyle, 1997)

$$
\begin{aligned}
\hat{T}_b^e &= -\frac{1}{2}\omega^2 \left(\int_0^l \rho I K_2 \hat{\theta}^2 dx + \int_0^l \rho A \hat{v}^2 dx \right) \\
\hat{U}_b^e &= \frac{1}{2} \int_0^l EI \left(\frac{d\hat{\theta}}{dx} \right)^2 dx + \frac{1}{2} \int_0^l GAK_1 \left(\frac{d\hat{v}}{dx} - \hat{\theta} \right)^2 dx
\end{aligned}
\tag{20}
$$

The potential energy due to the applied nodal forces is $\hat{V}_b^e = \hat{\mathbf{F}}_b^{e,T} \hat{\mathbf{q}}_b^e$, with $\hat{\mathbf{F}}_b^e = [\hat{V}_1 \quad \hat{M}_1 \quad \hat{V}_2 \quad \hat{M}_2]^T$.

The total sum of the energies ($\hat{U}^e = \hat{T}_b^e + \hat{U}_b^e$) and the potential energy ($\hat{V}_b^e$) are minimized with respect to the generalized degrees of freedom ($\hat{q}_{b,i}^e$) to obtain the dynamic stiffness matrix $\hat{\mathbf{K}}_b^D$

$$\hat{\mathbf{F}}_b^e = \hat{\mathbf{K}}_b^D \hat{\mathbf{q}}_b^e, \quad \hat{\mathbf{K}}_b^D = \hat{\mathbf{K}}_b^e - \omega^2 \hat{\mathbf{M}}_b^e \tag{21}$$

$\hat{\mathbf{M}}_b^e$ and $\hat{\mathbf{K}}_b^e$ are square matrices. These matrices and their detailed derivation can be found in Doyle (1997).

4 Bessel-based dynamic stiffness method

When the cross-section of a structural element is not constant, the differential equation that governs its displacements has variable coefficients. In general, papers about structural elements with variable cross-section consider only simple elements. For example, the exact solution of the differential equation of a simple bar with polynomial varying cross-section can be obtained using Bessel functions. When the variation is linear, the solution can be written in an exponential form, which is similar to the constant cross-section case (Banerjee & Williams, 1985). The exact solution for Euler-Bernoulli beams can also be expressed in Bessel functions terms (Banerjee & Williams, 1985; Petersson & Nijman, 1998). Due to its relative simplicity, in this paper only the Euler-Bernoulli beam will be considered. This fact will not affect the numerical comparison because the structural elements are not short.

4.1 Euler-Bernoulli beam element

The differential equation of a tapered Euler-Bernoulli beam is

$$\frac{\partial^2}{\partial x^2} \left(EI(x) \frac{\partial^2 v(x,t)}{\partial x^2} \right) + \rho A(x) \frac{\partial^2 v(x,t)}{\partial t^2} = 0 \tag{22}$$

A and I are both the area and the second moment of area of the variable cross-section, respectively

$$A(x) = A_1 \left(1 + \delta \frac{x}{L}\right)^n, \quad I(x) = I_1 \left(1 + \delta \frac{x}{L}\right)^{n+2} \tag{23}$$

After changing variables $\xi = 1 + \delta \frac{x}{L}$ and considering harmonic vibrations $v(\xi, t) = \overline{v}(\xi) sen(\omega t)$

$$\xi^2 \frac{d^4 \overline{v}}{d\xi^4} + 2(n+2)\xi \frac{d^3 \overline{v}}{d\xi^3} + (n+2)(n+1)\frac{d^2 \overline{v}}{d\xi^2} - \frac{\lambda_1^4}{\delta^4}\overline{v} = 0 \tag{24}$$

with $\lambda_1 = L \sqrt[4]{\frac{\rho A_1 \omega^2}{EI_1}}$, which has a solution given by

$$\overline{v}(\xi) = \frac{1}{\phi^n} \left(\overline{A}J_n(\phi) + \overline{B}Y_n(\phi) + \overline{C}I_n(\phi) + \overline{D}K_n(\phi)\right) \tag{25}$$

with $\phi = \frac{2\lambda_1}{\delta}\sqrt{\xi}$. J, Y, I and K are Bessel functions of the first, second, first modified and second modified kind, respectively. Using Eq. 25 it is possible to obtain the bending rotation $\overline{\theta}$, the bending moment $\overline{M}$ and the shear force $\overline{V}$ (Banerjee & Williams, 1985).

The displacement boundary conditions are

$$
\begin{array}{ll}
\text{At} \;\; x = 0 \;\; (\xi = 1), & \overline{v} = \overline{v}_1 \;\; \text{and} \;\; \overline{\theta} = \overline{\theta}_1 \\
\text{At} \;\; x = L \;\; (\xi = 1 + \delta), & \overline{v} = \overline{v}_2 \;\; \text{and} \;\; \overline{\theta} = \overline{\theta}_2
\end{array} \tag{26}
$$

Substituting this conditions in the equations for $\overline{v}$ and $\overline{\theta}$, it is obtained $\overline{\mathbf{q}}_b^e = \mathbf{B}\mathbf{A}$ with $\overline{\mathbf{q}}_b^e = [\overline{v}_1 \;\; \overline{\theta}_1 \;\; \overline{v}_2 \;\; \overline{\theta}_2]^T$ and $\mathbf{A} = [\overline{A} \;\; \overline{B} \;\; \overline{C} \;\; \overline{D}]^T$.

The force and moment boundary conditions are

$$
\begin{array}{ll}
\text{At} \;\; x = 0 \;\; (\xi = 1), & \overline{V} = \overline{V}_1 \;\; \text{and} \;\; \overline{M} = -\overline{M}_1 \\
\text{At} \;\; x = L \;\; (\xi = 1 + \delta), & \overline{V} = -\overline{V}_2 \;\; \text{and} \;\; \overline{M} = \overline{M}_2
\end{array} \tag{27}
$$

Substituting this conditions in the equations for $\overline{V}$ and $\overline{M}$, it is obtained $\overline{\mathbf{F}}_b^e = \mathbf{C}\mathbf{A}$ with $\overline{\mathbf{F}}_b^e = [\overline{V}_1 \;\; \overline{M}_1 \;\; \overline{V}_2 \;\; \overline{M}_2]^T$ and $\mathbf{A} = [\overline{A} \;\; \overline{B} \;\; \overline{C} \;\; \overline{D}]^T$.

The relationship between the forces vector and the displacements vector is $\overline{\mathbf{F}}_b^e = \overline{\mathbf{K}}_b^D \overline{\mathbf{q}}_b^e$, with $\overline{\mathbf{K}}_b^D$ as the dynamic stiffness matrix of an Euler-Bernoulli beam

$$\overline{\mathbf{K}}_b^D = \mathbf{C}\mathbf{B}^{-1} \tag{28}$$

5 Numerical example

In order to compare the above discretization methods, it was considered an asymmetric T-beam structure that has already been used in other works (Ahmida, 2001; Szwerc et al, 2000). The material is Lexan® (thermoplastic), $E = 2.62 \times 10^9 \, \text{N/m}^2$, $\rho = 1240 \, \text{kg/m}^3$, $\eta = 0.01$ and $\nu = 0.25$. To describe the material dissipation it was used the complex modulus model $E^* = E(1 + i\eta)$ (Coronado et al, 2002).

The T-beam structure is shown in Fig. 4. This structure has displacements in the $x - y$ plane only. The excitation force is harmonic, which can be written in exponential notation as $Fe^{i\omega t}$, in this work $F = 1$ N. Besides, the boundary conditions are *free* to simulate an aeronautical structure.

In order to compare the FEM, the SEM and the Bessel-based method, the leg 1 will have either constant or variable cross-section. Conversely, the legs 2 and 3 will always be discretized using the SEM as constant cross-section elements.

In this sense, it is important to stress that this comparison do not has a definitive character because this subject is very wide and complex. Moreover, it must be emphasized the general character of the FEM, this fact will not be so evident in this work due to the specific character of this comparison. So the conclusions cannot be applied to other cases without a previous study.

Figure 5 shows the power frequency response when all the three legs have constant cross-section. Since the SEM gives an exact solution for rods and beams of constant cross-section, it is necessary only one element to discretize each leg. It is shown the power at nodes 1 and 2. The difference between these two quantities is related to the dissipated energy in the leg 1.

The first comparison is shown in Fig. 6. In this case, the leg 1, of constant cross-section, is discretized using either the FEM or the SEM with only one element. The difference between the two methods is easily noted
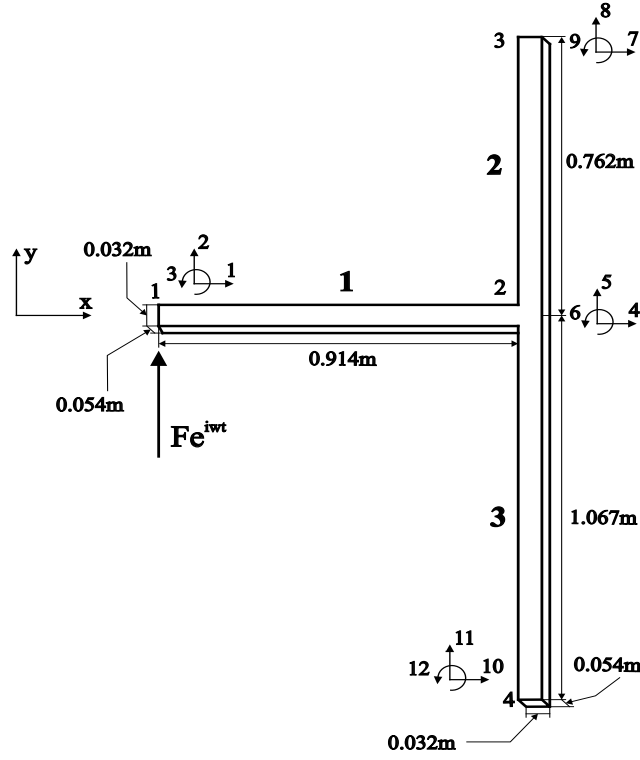
Figure 4. Asymmetric T-beam structure.

above the third resonance. To improve the results obtained using the FEM, the number of elements is increased from one to three, Fig. 7. In this case, the two methods show good agreement up to 200 Hz. From these two figures, it is easily verified that the SEM has some advantage over the FEM since the former requires less elements to suitably describe a structure with constant cross-section members. This results can be explained by the fact that at high frequencies the number of modes involved in the response increases, so the discretization must be refined to account for the higher complexity.

In Fig. 8, the height of the leg 1 cross-section varies linearly until $h_2 = 2h_1$. It is compared the SEM with the Bessel-based method. It is easily noted the poor responses obtained using the SEM with only one element. Additionally, negative power was obtained at some frequencies, so it was plotted only the absolute value. Conversely, the Bessel-based method needs only one element to obtain good responses at any frequency. Using the SEM with three elements, Fig. 9, it is obtained a better correspondence between the two methods.

In Fig. 10, the leg 1 is discretized using the FEM with one element. It can be noted that this method do not present great variations with respect to the Bessel-based method. Moreover, the FEM do not produce responses without physical meaning, like negative power, for example. Using the FEM with three elements, Fig. 11, the response is very similar to the Bessel-based method response.

To verify the correspondence between the SEM and the FEM, it is showed the Fig. 12. Finally, it is compared the response obtained by the Bessel-based method using two elements with the response obtained by the SEM using three elements, Fig. 13. The response obtained using the Bessel-based method degenerates when more than one element is used to discretize the leg 1, probably due to numerical errors calculating the stiffness matrix.

6 Conclusions

From the figures above discussed, it can be concluded that although the responses obtained, for appropriated discretizations, using the FEM and the SEM are very similar, the FEM appeared to be more reliable for coarse meshes. On the other hand, considering the FEM, the elements of the mass and the stiffness matrices obtained in this work are very complex, this fact produces slowness when the FEM is used, in some cases it was up to twice slow than the SEM case, for the same discretization level.

The literature is rich with papers about tapered beams. In general, this works compare only either the elements of the dynamic stiffness matrices or the time response (displacement or velocity). So it is not possible to see the problems found when the frequency response is calculated.

7   References

Ahmida, K.M., 2001, "Dynamic analysis of trusses at mid and high frequencies", (In portuguese), D.Sc. Thesis, Universidade Estadual de Campinas, Brazil.

Banerjee, J. and Williams, F., 1985, "Exact Bernoulli-Euler dynamic stiffness matrix for a range of tapered beams", International Journal for Numerical Methods in Engineering, Vol. 21, pp. 2289-2302.

Bathe, K.J., 1996, "Finite Element Procedures", Prentice Hall.

Corn, S., Bouhaddi, N. and Piranda, J., 1997, "Transverse vibrations of short beams: Finite element models obtained by a condensation method", Journal of Sound and Vibration, Vol. 201, No. 3, pp. 353-363.

Coronado, A., Trindade, M.A. and Sampaio, R., 2002, "Frequency-dependent viscoelastic models for passive vibration isolation systems", Shock and Vibration, Vol. 9, No. 4-5, pp. 253-264.

Coronado-Matutti, A., 2003, "Geometric optimization of a T-beam structure", (In portuguese), D.Sc. Thesis, PUC-Rio, Brazil.

Davis, R., Henshell, R.D. and Warburton, G.B., 1972, "A Timoshenko beam element", Journal of Sound and Vibration, Vol. 22, pp. 475-487.

Dawe, D.J., 1978, "A finite element for the vibration analysis of Timoshenko beams", Journal of Sound and Vibration, Vol. 60, No. 1, pp. 11-20.

Doyle, J.F., 1997, "Wave propagation in structures: Spectral analysis using Fast Discrete Fourier transforms", Springer-Verlag.

Langthjem, M. and Sugiyama, Y., 1999, "Optimum shape design against flutter of a cantilevered column with an end-mass of finite size subjected to a non-conservative load", Journal of Sound and Vibration, Vol. 226, No. 1, pp. 1-23.

Petersson, B. and Nijman, E., 1998, "The one-dimensional bending wave counterpart to the acoustic horn and the semi-infinite wedge", Journal of Sound and Vibration, Vol. 211, No. 1, pp. 95-121.

Rao, S.S. and Gupta, R.S., 2001, "Finite element vibration analysis of rotating Timoshenko beams", Journal of Sound and Vibration, Vol. 242, No. 1, pp. 103-124.

Reddy, J.N., 1984, "Energy and variational methods in applied mechanics", John Wiley & Sons.

Szwerc, R.P., Burroughs, C.B., Hambric, S.A. and McDevitt, T.E., 2000, "Power flow in coupled bending and longitudinal waves in beams", J. Acoust. Soc. Am., Vol. 107, No. 6, pp. 3186-3195.

Yokoyama, T., 1994, "A reduced integration Timoshenko beam element", Journal of Sound and Vibration, Vol. 169, No. 3, pp. 411-418.
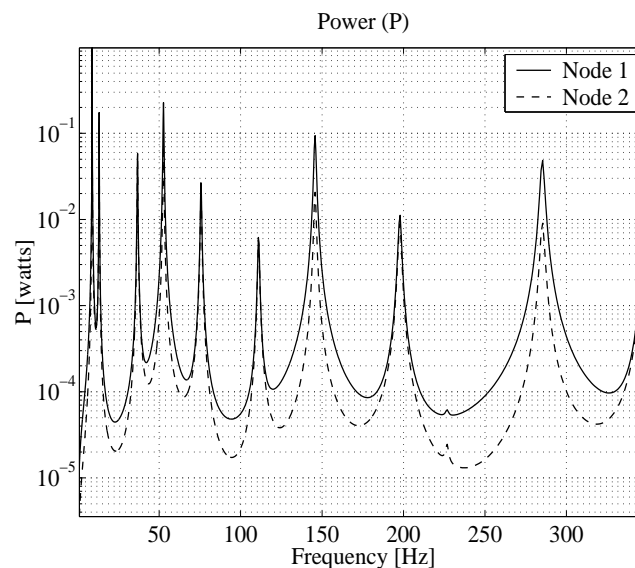
8   Copyright Notice

Figure 5. Power at nodes 1 and 2, leg 1 of constant cross-section discretized by the SEM (1 element).
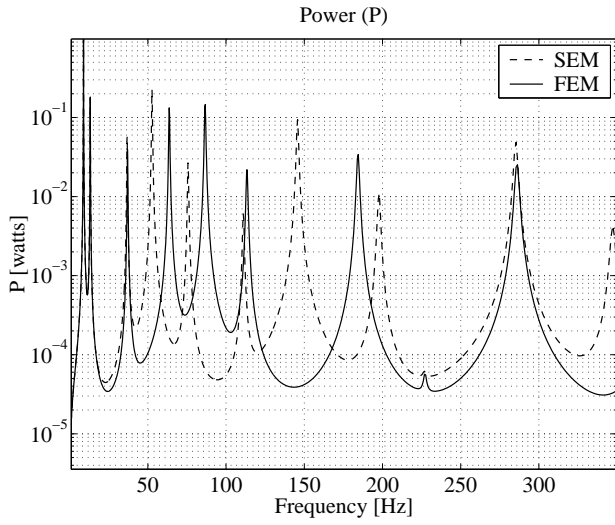
Figure 6. Power at node 1, leg 1 of constant cross-section discretized by either the SEM (1 element) or the FEM (1 element).
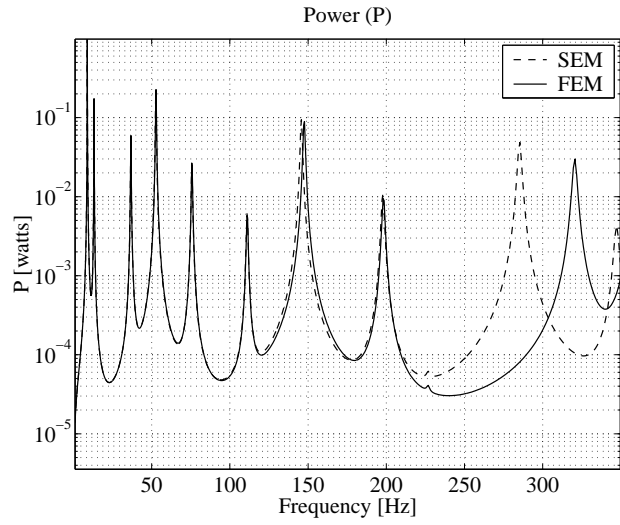

Figure 7. Power at node 1, leg 1 of constant cross-section discretized by either the SEM (1 element) or the FEM (3 elements).
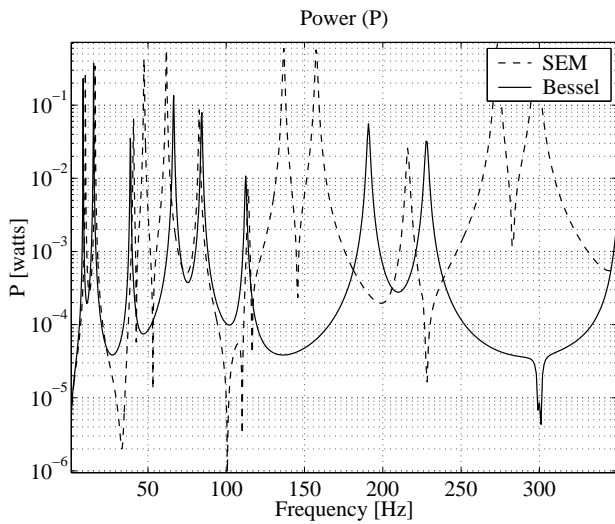

Figure 8. Power at node 1, leg 1 of variable cross-section ($h_2 = 2h_1$) discretized by either the SEM (1 element) or the Bessel-based method (1 element).
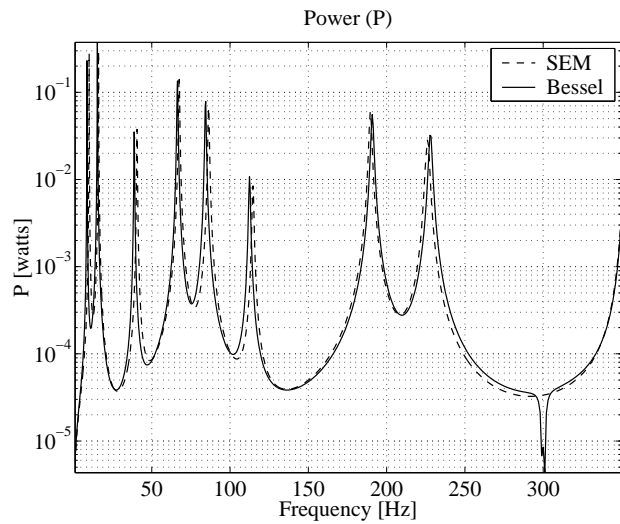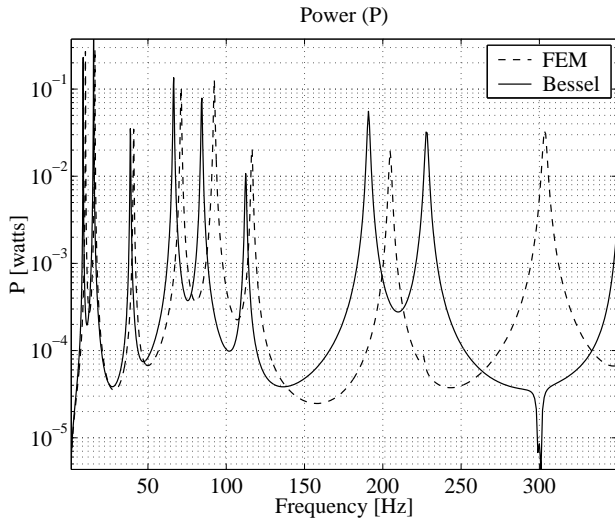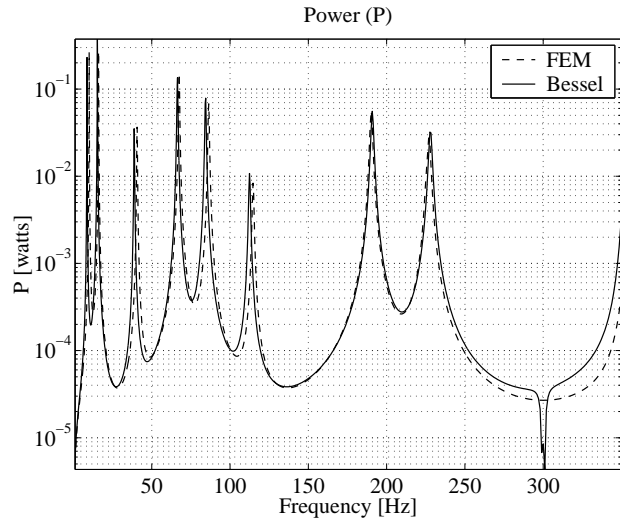

Figure 9. Power at node 1, leg 1 of variable cross-section ($h_2 = 2h_1$) discretized by either the SEM (3 elements) or the Bessel-based method (1 element).

Figure 10. Power at node 1, leg 1 of variable cross-section ($h_2 = 2h_1$) discretized by either the FEM (1 element) or the Bessel-based method (1 element).

Figure 11. Power at node 1, leg 1 of variable cross-section ($h_2 = 2h_1$) discretized by either the FEM (3 elements) or the Bessel-based method (1 element).
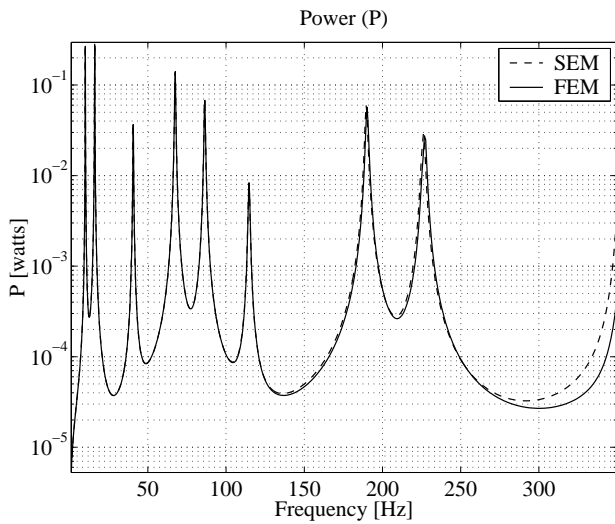

Figure 12. Power at node 1, leg 1 of variable cross-section ($h_2 = 2h_1$) discretized by either the SEM (3 elements) or the FEM (3 elements).
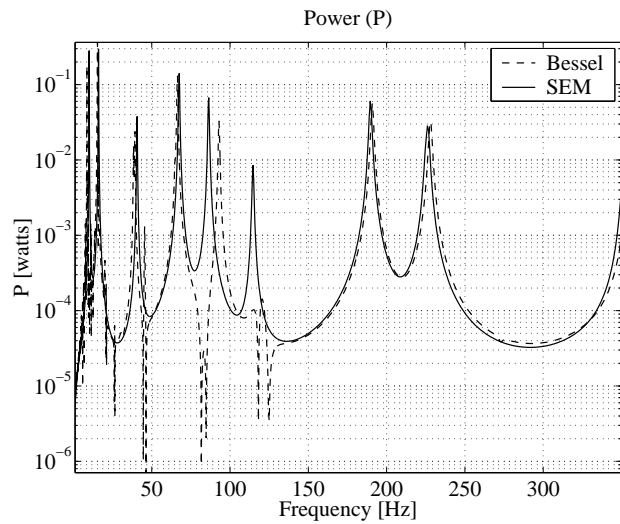
Figure 13. Power at node 1, leg 1 of variable cross-section ($h_2 = 2h_1$) discretized by either the Bessel-based method (2 elements) or the SEM (3 elements).